BUTTERWORTH HEINEMANN

Polymer Vol. 36 No. 14, pp. 2675–2680, 1995

0032-3861/95/$10.00+0.00

polymer papers

Time to frequency domain transforms

S. Havriliak Jr*
Rohm and Haas Research, Bristol Research Park, PO Box 219, Bristol, PA 19007, USA

and S. J. Havriliak
Havriliak Software Development Co., Huntingdon Valley, PA 19006, USA
(Received 20 June 1994; revised 3 December 1994)

Recently, Weiss *et al.* proposed an improved computational method for transforming the stretched exponential function from the time domain to the frequency domain. In this work, we report another simpler and more general transform technique based on Schwarzl's methodology for transforming data from the time domain to the frequency domain. Rather than assume a doubling in the frequency spacing as does Schwarzl, the optimum spacing is determined by non-linear methods. This technique, or extended Schwarzl method, yields results on the stretched exponential that are comparable to the more standard high quality results obtained by Koizumi and Kita as well as Dishon *et al.* Comparisons show that the real parts of the complex numbers are within a few digits in the sixth decimal place, while the imaginary numbers are within a few digits in the fourth decimal place. One advantage to the method described herein is that it can be used to transform any smoothly decaying (or rising) time function on a personal computer of modest dimensions.

(Keywords: time to frequency transforms; Schwarzl's method; stretched exponential)

INTRODUCTION

In a recent paper by Weiss *et al.*[1], they proposed an improved computational method for transforming the stretched exponential or the Kohlrausch–Williams–Watts (KWW)[2–4] function from the time domain to the frequency domain. The KWW function is given by the following expression:

$$\epsilon(t) = \exp\left[-(t/\tau_0)^k\right]$$

In this expression $\epsilon(t)$ is the time dependent dielectric constant at time t, τ_0 is the relaxation time and k is the KWW parameter. Often it is desirable to transform the KWW results from the time ($\epsilon(t)$) domain to the frequency ($\epsilon^*(\omega)$) domain. The quantity $\epsilon^*(\omega)$ is the complex dielectric constant at radian frequency ω and is related to the real ($\epsilon'(\omega)$) and imaginary ($\epsilon''(\omega)$) parts through $\epsilon^*(\omega) = \epsilon'(\omega) - \epsilon''(\omega)$. Although these transforms may be considered as straightforward Fourier transform problems, they are very difficult to carry out because of serious numerical or convergence problems. In other words, the infinite Fourier series does not readily converge.

The elegant convergence-accelerating methods of Weiss *et al.* were applied to series expansions for the stable law density given by

$$Q_k(z) = \frac{1}{\pi}\int_0^\infty \exp\left[-(u)^k\right]\cos(zu)\,du \qquad (1a)$$

and

$$V_k(z) = \frac{1}{\pi}\int_0^\infty \exp\left[-(u)^k\right]\sin(zu)\,du \qquad (1b)$$

In these expressions $z = \omega\tau$, where τ is the relaxation time, and the product z ranges from 0 to ∞. The parameter k was defined above and ranges from 0 to 1. The quantities $Q_k(z)$ and $V_k(z)$ are related to the real and imaginary parts of the complex dielectric constant (see equations (3) elsewhere[1]). Finally, u is an intermediary parameter used in the transform and need not concern us here.

The purpose of this work is to report a simpler method for accomplishing the same ends and one that is more general since it is not limited to the KWW function but is applicable to any time decay function. First, we shall review the pertinent background literature before discussing the results.

BACKGROUND

Formally, these problems were solved by Gross with his contributions to linear response theory[5]. In this discussion we consider the dielectric case only; the one for viscoelasticity is mathematically almost identical. Following Gross's line of development, we can define the time dependent dielectric constant $\epsilon(t)$ in terms of a linear integral

$$\epsilon(t) = \epsilon_\infty + \int_0^\infty G(\tau)[1 - \exp(-t/\tau)]\,d\tau \qquad (2)$$

where ϵ_∞ is the instantaneous dielectric constant, $G(\tau)$ is the distribution of relaxation times and the term $[1 - \exp(-t/\tau)]$ represents the Debye response of a viscosity-damped system to a unit step if the electric field is suddenly applied at $t = 0$. The real and imaginary components of the frequency dependent

* To whom correspondence should be addressed

dielectric constant are obtained by taking the Laplace transform of equation (2)

$$\epsilon'(\omega) = \epsilon_0 + \int_0^\infty G(\tau)\left(\frac{1}{1+\omega^2\tau^2}\right) d\tau \quad (3)$$

$$\epsilon''(\omega) = \int_0^\infty G(\tau)\left(\frac{\omega\tau}{1+\omega^2\tau^2}\right) d\tau \quad (4)$$

Schwarzl and Struik[6] have shown that the application of these integral transformations to experimental data gives rise to a few basic difficulties. Later, Schwarzl[7] reported an efficient algorithm for transforming experimental data between the frequency and time domains. The only constraint imposed on the data by his analysis is that they must be sampled at even (doubling) time intervals. Peak transform errors associated with Schwarzl's algorithm were reported to be approximately 0.8%. Although these errors are usually regarded as acceptable, particularly within the viscoelastic context in which they were developed, they can be improved upon significantly.

The key to Schwarzl's analysis rests in remembering the properties of a quantity called the finite difference function, $\epsilon(2\alpha t) - \epsilon(\alpha t)$, defined by equation (5), and certain relationships that exist between other quantities, called intensity functions, $I_{\text{time}}(x)$, $I_{\text{real}}(x)$, $I_{\text{imag}}(x)$ and $I_{\text{diff}}(\alpha, x)$, defined by equations (6)–(9), respectively. The finite difference function is obtained from equation (2) by taking the difference between the dielectric constants defined by equation (2) and evaluated at different times or

$$\epsilon(2\alpha t) - \epsilon(\alpha t) = \int_0^\infty G(\tau)[\exp(-\alpha\tau/t) - \exp(-2\alpha\tau/t)]\, d\tau \quad (5)$$

Equations (2)–(5) are similar; they are integrals containing a distribution of relaxation times multiplied by a function of either $\omega\tau$ or t/τ. Following Schwarzl, this second function (not the distribution of relaxation times) is referred to as the intensity function. Introducing a new variable ($x = t/\tau$ and $x = 1/\omega\tau$), the intensity functions in equations (2)–(5) become

$$I_{\text{time}}(x) = 1 - \exp(-x) \quad (6)$$

$$I_{\text{real}}(x) = \frac{x^2}{1+x^2} \quad (7)$$

$$I_{\text{imag}}(x) = \frac{x}{1+x^2} \quad (8)$$

$$I_{\text{diff}}(\alpha, x) = \exp(-\alpha x) - \exp(-2\alpha x) \quad (9)$$

The fundamental relationships between the intensity functions defined in equations (6)–(9) are

$$I_{\text{time}}(x) - I_{\text{real}}(x) = \frac{1}{1+x^2} - \exp(-x) \approx \sum_{T=1}^{NT(\text{real})} c_T I_{\text{diff}}(a_T, x) \quad (10)$$

$$I_{\text{imag}}(x) = \frac{x}{1+x^2} \approx \sum_{T=1}^{NT(\text{imag})} c_T I_{\text{diff}}(a_T, x) \quad (11)$$

These observations suggest that $I_{\text{time}}(x) - I_{\text{real}}(x)$ can be represented by the series expansion given in equation (10) if the expansion coefficients and exponents are chosen in a sensible way. In the Appendix a least-squares regression procedure is given to accomplish this task. Multiplying equations (10) and (11) by $G(\tau)$ and integrating with respect to τ from 0 to ∞ gives

$$\epsilon_{\text{real}}(\omega) = \epsilon_{\text{time}}\left(t = \frac{1}{\omega}\right) - \sum_{T=1}^{NT} c_T\left[\epsilon\left(t = \frac{2\alpha_T}{\omega}\right) - \epsilon\left(t = \frac{\alpha_T}{\omega}\right)\right] \quad (12)$$

$$\epsilon_{\text{imag}}(\omega) = \sum_{T=1}^{NT} c_T\left[\epsilon\left(t = \frac{2\alpha_T}{\omega}\right) - \epsilon\left(t = \frac{\alpha_T}{\omega}\right)\right] \quad (13)$$

These equations express the frequency dependent dielectric constant in terms of the time dependent dielectric constant. Time appears on the right-hand side of equations (12) and (13) as α_T/ω. These equations

Table 1 Expansion coefficients and exponents that define the transform from the time domain to the frequency domain

	Real results		Imaginary results	
Term	Coefficients	Exponents	Coefficients	Exponents
1	0.000 860 168	0.019 486 588	0.010 989 37	0.003 093 89
2	0.042 693 237	0.096 300 497	0.026 188 24	0.011 965 00
3	−0.092 314 353	0.124 263 918	0.058 669 47	0.032 101 96
4	0.105 192 317	0.161 240 684	0.131 534 36	0.077 293 24
5	0.401 541 678	0.527 912 944	0.287 550 33	0.177 931 48
6	−0.357 521 204	0.740 080 011	0.570 428 10	0.392 437 05
7	0.195 068 919	1.184 264 573	0.505 305 50	0.755 501 91
8	1.549 763 318	2.526 275 886	0.580 305 09	0.959 468 82
9	−1.390 185 203	3.459 325 677	0.812 369 41	1.803 736 98
10	0.391 478 144	4.645 071 706	−1.038 818 47	2.903 690 82
11	−0.013 857 341	8.207 585 333	0.423 347 95	4.741 251 99
12			−0.127 603 42	7.327 571 14
13			0.028 148 00	11.265 943 59
14			−0.003 838 90	17.029 468 23

differ from Schwarzl's in content only, not form. These parameters were evaluated using non-linear regression methods (see the Appendix) and the results are listed in *Table 1*. These parameters are used in exactly the same way as are the Schwarzl parameters. We refer to this method as the extended Schwarzl method. The difference between the two methods is that the frequency (or time) increments are not uniformly spaced and consequently the intensity parameters are different. The times are, however, efficiently or strategically spaced as required by non-linear regression methods. In the event that only uniformly spaced data are available for transformation, a spline routine must be employed.

APPLICATION TO THE KWW FUNCTION

Another variation of the KWW function is given by

$$\epsilon_n(t) = \frac{\epsilon(t) - \epsilon_i}{\epsilon_0 - \epsilon_i} = 1 - \exp[-(t/t_0)^k] \qquad (14)$$

In this expression, $\epsilon_n(t)$ is the normalized time dependent dielectric constant from the sudden application of a constant electric field to the test specimen at time $t = 0$, k is the KWW parameter and t_0 is the relaxation time. First, we use equation (14) to calculate $\epsilon_n(t)$ as a function of t over a parameter k range of 0.3–1.0. Then we transform $\epsilon_n(t)$ to $\epsilon_n^*(\omega)$ using the methods of the previous section. Finally, we compare these results with those of other and more established methods.

Koizumi and Kita[8] transformed the time dependent dielectric constant calculated from the stretched exponential function for given values of k between 0.29 and 1.0 and incremented by 0.01. Dishon *et al.*[9] also treated the same problem but did not mention the results of Koizumi and Kita. Their procedure was similar and care was taken to ensure convergence. Their results are reported to six decimal places. They covered a similar parameter and time range as did Koizumi and Kita. Plots of $\log \epsilon''(\omega)$ vs. log(frequency) are given in *Figure 1* for the results of Koizumi and Kita, Dishon *et al.*, the extended Schwarzl method and the unaltered Schwarzl method. The calculations were carried out for $k = 0.3$. The frequency range was limited to the region of the loss maximum. The simple results of Schwarzl are about 0.2% from the results obtained from the tedious computations of the other two methods, while the results of the extended Schwarzl method are indistinguishable from the results of the series methods in these plots.

These overlay plots are a poor method for comparing results; a residual plot is to be preferred. Residual plots for $\epsilon'(\omega)$ and $\epsilon''(\omega)$, defined as the differences between the extended Schwarzl and Koizumi and Kita or Dishon *et al.* methods, are given in *Figures 2* and *3*. The differences for $\epsilon'(\omega)$ have been multiplied by 10^6, and for $\epsilon''(\omega)$ the differences have been multiplied by 10^4. Plots of the residuals with $\log f$ for various b are given in *Figure 4*. If we define σ' as the root mean square real error, then the value for σ' is found to depend on b with a

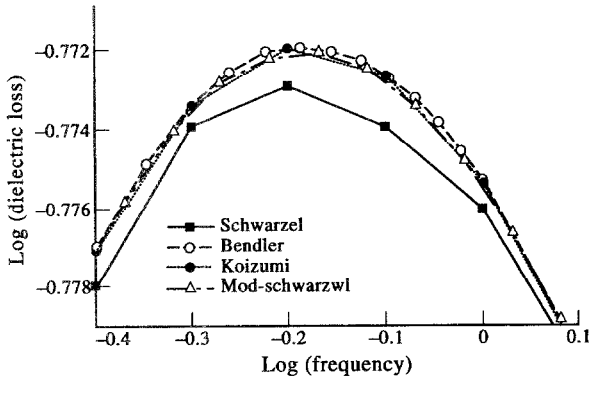

Figure 1 Plots of $\log \epsilon''(\omega)$ vs. log(frequency) for $k = 0.3$ in the vicinity of the loss maximum

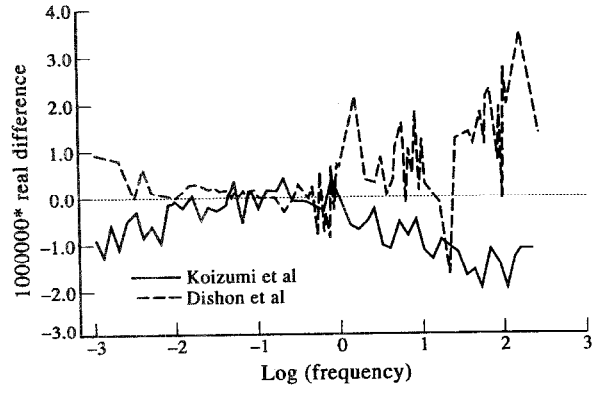

Figure 2 Plots of 10^6 times the differences between the $\epsilon'(\omega)$ values calculated from the extended Schwarzl, Koizumi and Kita and Dishon *et al.* methods for $k = 0.3$

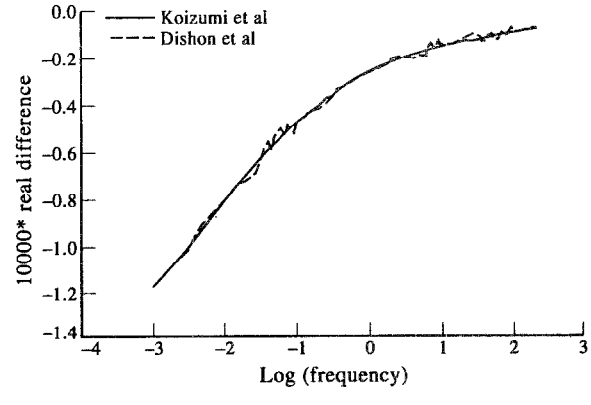

Figure 3 Plots of 10^4 times the differences between the $\epsilon''(\omega)$ values calculated from the extended Schwarzl, Koizumi and Kita and Dishon *et al.* methods for $k = 0.3$

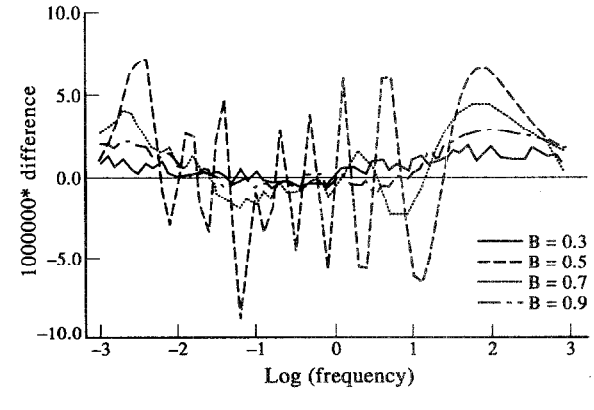

Figure 4 Plots of 10^6 times the differences between the $\epsilon''(\omega)$ values calculated from the extended Schwarzl and Koizumi and Kita methods for the values of b listed

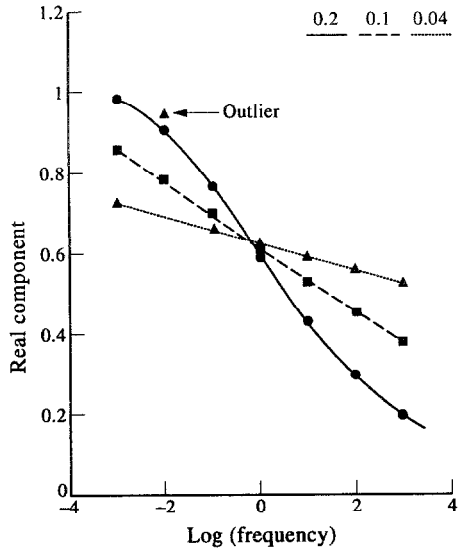

Figure 5 Plots of $\epsilon'(\omega)$ for the k values shown in the legend. In all cases the lines represent data from the modified Schwarzl method, while the symbols represent data from Dishon *et al.* The point represented as an outlier is from an apparent error in $V_k(z)$

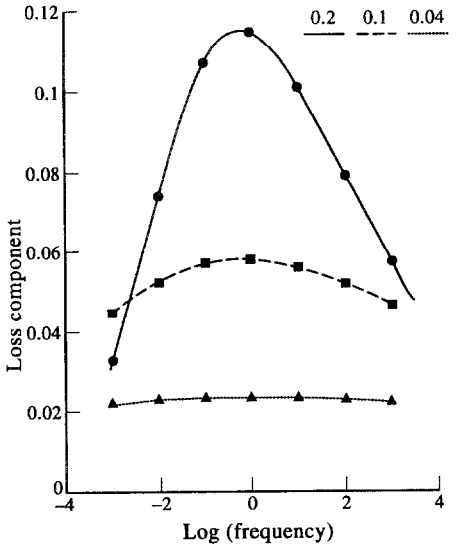

Figure 6 Plots of $\epsilon''(\omega)$ for the k values shown in the legend. In all cases the lines represent data from the modified Schwarzl method, while the symbols represent data from Dishon *et al.*[9]

maximum value of $\sigma' = 4 \times 10^{-6}$ for $k = 0.9$ and $\sigma'(\omega) = 0.9 \times 10^{-6}$ for $k = 0.3$. The values for σ'' are about 100 times higher.

CONCLUSIONS

The extended Schwarzl method should be useful to many scientists because the calculations can be carried out on a personal computer (PC) of modest dimensions. For the specific cases described here, the transforms were carried out on a Compaq PC operating at 25 MHz with 4 Mbytes of random access memory and MATHCAD as a software routine. Typical transforms using 200 data points were carried out in less than one minute. The most important point is, however, that the results of the extended Schwarzl method agree with the results of the more straightforward methods to a few digits in the sixth

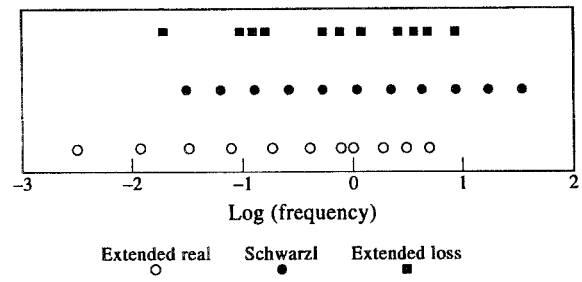

Figure 7 Spacings for the Schwarzl and extended Schwarzl methods

decimal place for $\epsilon'(\omega)$ and a few digits in the fourth decimal place for $\epsilon''(\omega)$. It should be pointed out that there are three regions where the values of $\epsilon^*(\omega) - \epsilon_\infty \rightarrow 0$, i.e. the high frequency end of the $\epsilon'(\omega)$ curve and the high and low frequency ends of the $\epsilon''(\omega)$ curve. In such cases the differences between the various studies will be a significant percentage. In other words, if the region of comparison in the $\epsilon''(\omega)$ curve from one method ($k = 0.3$ and $\omega = 0.001$) is 0.008 8966, from the other study it is 0.008 7825. The difference is 0.000 1141 with an error of 1.3% but $\sigma'' = 0.000\,1141$, which is within the stated error. Similar estimates near the loss maximum yield a difference of 0.01%. The reason for representing the differences between the various methods in terms of σ rather than a percentage is that the former is approximately constant over a range of k and ω values, while the latter will vary by several orders of magnitude.

A number of points worthy of note should be made for low k values. Overlay plots for k values of 0.2, 0.1 and 0.04 are given in *Figure 5* for the real part and in *Figure 6* for the imaginary part. The differences between the present results and those of Dishon *et al.* are about the same as they are for the larger values of k. In the case of the real part, the curves are rotating about their midpoints, so that there is no serious reduction in transform accuracy in the frequency interval of ± 3. However, in the same frequency and parameter interval the loss is reducing in value to about 0.02. Since the precision affects by several digits in the fourth decimal place, the difference between the two studies may be a few per cent. The point to be made here is that the user of these methods should be aware of these limitations.

It is also of interest to compare graphically the frequency spacings in this work with those in the method of Schwarzl. This is shown in *Figure 7*. Finally, the frequency range can be readily extended from six to 12 decades with little increase in computer time. Although we have made no attempt to verify this point, it does seem reasonable to conclude that these transforms can be performed in hand-held calculators like those manufactured by Hewlett–Packard or Texas Instruments.

REFERENCES

1 Weiss, G. H., Dishon, M., Long, A. M., Bendler, J. T., Jones, A. A., Inglefield, P. T. and Bandis, A. *Polymer* 1994, **35**, 1880
2 Kohlrausch, R. *Pogg. Ann. Phys. Chem.* 1854, **91**, 179
3 Kohlrausch, F. *Pogg. Ann. Phys. Chem.* 1863, **119**, 337
4 Williams, W. and Watts, D. C. *Trans. Faraday Soc.* 1970, **66**, 80
5 Gross, B. 'Mathematical Structure of the Theories of Viscoelasticity', Hermann, Paris, 1953
6 Schwarzl, F. R. and Struik, L. C. E. *Adv. Mol. Relax. Process.* 1967, **1**, 201

7 Schwarzl, F. R. *Rheol. Acta* 1969, **8**, 6
8 Koizumi, N. and Kita, Y. *Bull. Inst. Chem. Res., Kyoto Univ.* 1978, **56**, 300
9 Dishon, M., Weiss, G. H. and Bendler, J. T. *J. Res. Nat. Bur. Stand.* 1985, **90**, 27
10 Bates, D. M. and Watts, D. G. 'Nonlinear Regression Analysis and Its Applications', Wiley, New York, 1988

APPENDIX

Regression analysis

Here we describe the regression techniques that were used to evaluate the expansion coefficients and exponents listed in *Table 1*. The advantages of evaluating the expansion coefficients and exponents in this way are three-fold. The first advantage is that the transformation errors associated with equations (12) and (13) are roughly a factor of 500 times smaller than those originally reported by Schwarzl. The second advantage is that the breadth of the transformed data (maximum (transform variable) − minimum (transform variable)) will always be larger with our values of the expansion coefficients and exponents. This larger breadth is an artifact of the regression analysis; the regression forces the exponents closer together than the fitting algorithm originally used by Schwarzl. Since the exponents determine the width of the interval that gets mapped into a single point in the transform domain, our more tightly packed exponents produce a broader range of transformed data. The third consequence of the regression analysis is that the exponents will no longer be integers; hence, application of equations (12) and (13) will require chaotically spaced times. This, of course, adds another step to the data transformation; the data must first be splined so that they may be interpolated while applying the transform equations. However, using overdetermined splines* can also lead to significant noise reduction in the transformed data.

The expansion coefficients and exponents used to define the approximate intensity function in equations (10) and (11) can be determined from standard regression methods[10]. In what follows, we develop the regression equations used to determine the expansion coefficients and exponents for equation (10) only. Analogous expressions can be developed for equation (11). The expansion coefficients and exponents are obtained by minimizing a quantity called the regression function (RF), defined by

$$RF(c_1,\ldots,c_{NT},a_1,\ldots,a_{NT}) = \frac{1}{NP-NT-1}\sum_{P=1}^{NP} R_P^2(c_1,\ldots,c_{NT},a_1,\ldots,a_{NT}) \quad \text{(A1)}$$

This function is a least-squares regression function. It contains the sums of the squared distances between the exact and approximate intensity functions defined by equations (10) and (11). In this expression, NP is the number of points over which the squared distance or squared residual is calculated and NT is the number of terms in the approximate intensity function defined in equation (10). The quantity $RF(c_1,\ldots,c_{NT}, a_1,\ldots,a_{NT})$, called the residual evaluated at the point x_P, is defined as

$$R_P(c_1,\ldots,c_{NT},a_1,\ldots,a_{NT}) = I_{\text{real}}(x_P) - \sum_{T=1}^{NT} c_T I_{\text{diff}}(a_T,x_P) \quad \text{(A2)}$$

This residual is the difference between the exact and approximate intensity functions defined in equations (10) and (11). Since the residual is linear in the expansion coefficients c_T and non-linear in the exponential parameters a_T, each of the expansion coefficients depends parametrically on all the exponents. Hence, the regression function may be simplified as follows

$$RF(a_1,\ldots,a_{NT}) = \frac{1}{NP-NT-1}\sum_{P=1}^{NP} R_P^2(a_1,\ldots,a_{NT}) \quad \text{(A3)}$$

$$R_P(a_1,\ldots,a_{NT}) = I_{\text{real}}(x_P) - \sum_{T=1}^{NP} c_T(a_1,\ldots,a_{NT}) I_{\text{diff}}(a_T,x_P) \quad \text{(A4)}$$

The expansion coefficients can be related to the exponents by way of the constraint equation

$$\vec{c}(a_1,\ldots,a_{NT}) = M^{-1}(a_1,\ldots,a_{NT})\vec{b}(a_1,\ldots,a_{NT}) \quad \text{(A5)}$$

This equation can be verified by finding the equations that minimize the regression function $RF(c_1,\ldots,c_{NT}, a_1,\ldots,a_{NT})$ with respect to variations in the expansion coefficients only and solving for the expansion coefficients in terms of the exponents. Here, $\vec{c}(a_1,\ldots,a_{NT})$ is a column vector containing the expansion coefficients. The square matrix $M(a_1,\ldots,a_{NT})$ and the column vector $\vec{b}(a_1,\ldots,a_{NT})$ are defined by the matrix elements

$$M_{k,l}(a_1,\ldots,a_{NT}) = \sum_{P=1}^{NP} I_{\text{diff}}(a_k,x_P) I_{\text{diff}}(a_l,x_P) \quad \text{(A6)}$$

$$b_{k,l}(a_1,\ldots,a_{NT}) = \sum_{P=1}^{NP} I_{\text{real}}(x_P) I_{\text{diff}}(a_k,x_P) \quad \text{(A7)}$$

The expansion coefficients and exponents are obtained by minimizing $RF(a_1,\ldots,a_{NT})$ defined by equation (A3) with respect to all variations in the exponents a_T. This is done by expanding the regression function $RF(a_1,\ldots,a_{NT})$ in a Taylor series including terms through to second order. The Taylor series representation of the regression function is then minimized with respect to variations in the exponents. This procedure results in the following matrix equation that must be solved iteratively for the exponents

$$\vec{\Delta}(a_1,\ldots,a_{NT}) = -S^{-1}(a_1,\ldots,a_{NT})\vec{G}(a_1,\ldots,a_{NT}) \quad \text{(A8)}$$

Here, $S(a_1,\ldots,a_{NT})$ is an NT by NT square matrix of the second derivatives of the regression function $RF(a_1,\ldots,a_{NT})$ with respect to all pairs of exponents. The column vector $\vec{G}(a_1,\ldots,a_{NT})$ contains the NT first derivatives of the regression function with respect to all exponents, and the column vector $\vec{\Delta}(a_1,\ldots,a_{NT})$, also with NT elements, contains the displacements for each

* By overdetermined spline we mean one in which many more than two data points are used to define each term in a polynomial. This spline does not just 'connect the dots', but instead performs signal averaging

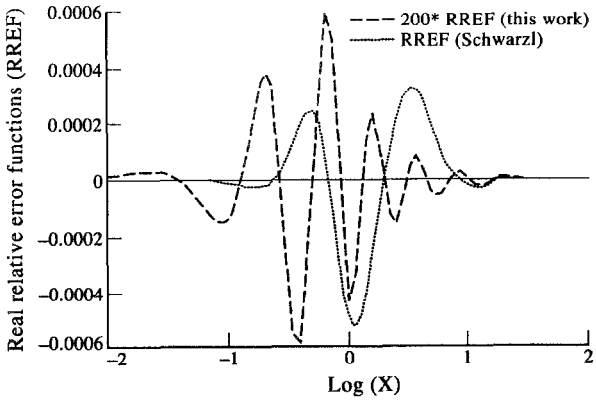

Figure 8 Plots of the imaginary residuals vs. log(frequency) for the two methods given here. Note that the residuals from the present study have been multiplied by 200

of the exponents that minimize the Taylor series representation of the regression function.

Results and discussion of errors

The results from the regression analyses are given in *Table 2*. The first and second rows list the quantities that gauge the quality of the fits obtained by using the regression function from the previous section. These are the root mean square residual (RMS(residual)) defined by equation (A9) and the maximum residual

Table 2 Statistics from the regression analyses for the expansion coefficients and exponents that define the Fourier transform

	Real results	Imaginary results
RMS(residual)	9.1×10^{-6}	4.4×10^{-6}
Max|residual|	20.5×10^{-6}	8.9×10^{-6}

(max|residual|)

$$RMS(\text{residual}) = \left[\frac{1}{NP - NT - 1} \times \sum_{P=1}^{NP} R_P^2(c_1, \ldots, c_{NT}, a_1, \ldots, a_{NT}) \right]^{1/2} \quad \text{(A9)}$$

The residual $R_P^2(c_1, \ldots, c_{NT}, a_1, \ldots, a_{NT})$ is defined by equation (A4) by using the expansion coefficients and exponents reported in *Table 1*. The maximum residual is the maximum value of the real residual $R_P(c_1, \ldots, c_{NT}, a_1, \ldots, a_{NT})$ defined by equation (A9) and a similar one for the imaginary residual evaluated over the range $x_P \in (-2, \ldots, +2)$. Plots of 200 times the imaginary residual from the extended Schwarzl method and the imaginary residual from the original Schwarzl method are given in *Figure 8*.